

QUT Digital Repository:
<http://eprints.qut.edu.au/>



Frost, Ray L. and Keefe, Eloise C. (2008) *Raman spectroscopic study of the schmiederite $Pb_2Cu_2[(OH)_4/SeO_3/SeO_4]$* . *Journal of Raman Spectroscopy*, 39(10). pp. 1408-1412.

© Copyright 2008 John Wiley & Sons

Raman spectroscopic study of the schmiederite $\text{Pb}_2\text{Cu}_2[(\text{OH})_4|\text{SeO}_3|\text{SeO}_4]$

Ray L. Frost* and Eloise C. Keeffe

Inorganic Materials Research Program, School of Physical and Chemical Sciences, Queensland University of Technology, GPO Box 2434, Brisbane Queensland 4001, Australia.

Abstract

Raman spectroscopy lends itself to the studies of selenites, selenates, tellurites and tellurates and related minerals. The mineral schmiederite $\text{Pb}_2\text{Cu}_2[(\text{OH})_4|\text{SeO}_3|\text{SeO}_4]$ is interesting in that both selenite and selenate anions occur in the structure.

Raman bands of schmiederite at 1095 and 934 cm^{-1} are assigned to the symmetric and antisymmetric mode of the $(\text{SeO}_4)^{2-}$ anions. For selenates and selenites, the symmetric stretching mode occurs at a higher position than the antisymmetric stretching mode, as is evidenced in the Raman spectrum of schmiederite. The band at 834 cm^{-1} is assigned to the symmetric $(\text{SeO}_3)^{2-}$ units. The two bands at 764 and 739 cm^{-1} are attributed to the antisymmetric $(\text{SeO}_3)^{2-}$ units. An intense sharp band at 398 cm^{-1} is assigned to this ν_2 bending mode. The two bands at 1576 and 1604 cm^{-1} are assigned to the deformation modes of the OH units. The observation of multiple OH bands supports the concept of a much distorted structure. This is based upon the four OH units coordinating the copper in a square planar structure. A single symmetric Raman band is observed at 3428 cm^{-1} and is assigned to the symmetric stretching mode of the OH units. The observation of multiple infrared OH stretching bands supports the concept of non-equivalent OH units in the schmiederite structure.

KEYWORDS: selenate, selenite, Raman spectroscopy, mandarinoite, schmiederite, chalcomenite, clinochalcomenite

INTRODUCTION

Selenites and tellurites may be subdivided according to formula and structure¹. There are five groups based upon the formulae (a) $\text{A}(\text{XO}_3)$, (b) $\text{A}(\text{XO}_3) \cdot x\text{H}_2\text{O}$, (c) $\text{A}_2(\text{XO}_3)_3 \cdot x\text{H}_2\text{O}$, (d) $\text{A}_2(\text{X}_2\text{O}_5)$ and (e) $\text{A}(\text{X}_3\text{O}_8)$. Of the selenites, molybdomenite is an example of type (a); chalcomenite, clinochalcomenite, cobaltomenite and ahlfeldite are minerals of type (b) mandarino is an example of type (c). There are no known examples of selenite minerals with formula (d) and (e). Examples of these groups may be found with tellurite minerals. Mandarino² reported that the oxysalts of the element selenium, selenites (with minerals containing Se^{4+}) and selenates (with minerals containing Se^{6+}) are very rare as minerals. Only fifteen selenium oxysalts are known to occur naturally; thirteen are so-called 'pure' selenites, i.e., they contain only selenite anionic groups. The other two minerals contain two anionic groups; in one case, selenate and sulfate, and in the other, selenate and selenite. A listing of the selenites is as follows: ahlfeldite, $\text{NiSeO}_3 \cdot 2\text{H}_2\text{O}$; chalcomenite and clinochalcomenite,

* Author to whom correspondence should be addressed (r.frost@qut.edu.au)

CuSeO₃·2H₂O; cobaltomenite, CoSeO₃·2H₂O; demesmaekerite, Pb₂Cu₅(UO₂)₂(SeO₃)₆(OH)₆·2H₂O; derriksite, Cu₄(UO₂)(SeO₃)₂(OH)₆; francisite, Cu₃Bi(SeO₃)₂O₂Cl; guilleminite, Ba(UO₂)₃(SeO₃)₂(OH)₄·3H₂O; haynesite, (UO₂)₃(OH)₂(SeO₃)₂·5H₂O; mandarinoite, Fe₂(SeO₃)₃·6H₂O; marthozite, Cu(UO₂)₃(SeO₃)₃(OH)₂·7H₂O; molybdomenite, PbSeO₃; and sphiite, Zn₂(SeO₃)Cl₂. The selenates are: olsacherite, Pb₂(SeO₄)(SO₄) and schmiederite, Pb₂Cu₂(OH)₄(SeO₄)(SeO₃). Of the selenites is the mineral chalcomenite and its dimorph clinochalcomenite. Chalcomenite, CuSeO₃·2H₂O, is a rare secondary mineral found in the oxidised deposits of Cu-Se bearing minerals. It is orthorhombic with point group 222²⁻⁴. The chalcomenite is dimorphous with the monoclinic clinochalcomenite⁵ and is normally found as powdery crusts or massive films with crystal growth along the (001) direction⁵.

Schmiederite Pb₂Cu₂[(OH)₄|SeO₃|SeO₄], is a monoclinic mineral^{2,6-9} and is light blue in appearance. The mineral is formed in the oxidised zone of selenium-bearing hydrothermal base metal deposits. Schmiederite can be associated with other selenite bearing minerals including chalcomenite, clinochalcomenite and molybdomenite. X-ray crystallographic analysis proves that the mineral schmiederite contains both selenite and selenate groups. The crystal structure is understood to be closely related to that of linarite⁹. Figure 1 displays a model of the schmiederite structure. The Pb atom in linarite and the Pb(1) atom in schmiederite each have 3 Pb-O bonds with trigonal pyramidal arranged ligands. The Pb(2) atom in schmiederite has only 1 such near O atom. The Cu atoms are approx. square planar coordinated by hydroxyl groups. In addition, 2 further O atoms complete the coordination to a strongly distorted octahedron.

Raman spectroscopy has proven very useful for the study of minerals¹⁰⁻¹⁴. Indeed, Raman spectroscopy has proven most useful for the study of diagenetically related minerals as often occurs with many minerals¹⁵⁻²⁵. Some previous studies have been undertaken by the authors, using Raman spectroscopy to study complex secondary minerals formed by crystallisation from concentrated sulphate solutions. The aim of this paper is to present Raman and infrared spectra of natural selected selenites and to discuss the spectra from a structural point of view. It is part of systematic studies on the vibrational spectra of minerals of secondary origin in the oxide supergene zone and their synthetic analogs.

EXPERIMENTAL

Minerals

The schmiederite samples originated from El Dragon Mine, Potosi, Bolivia. The clinochalcomenite also originated from El Dragon Mine, Potosi, Bolivia. The cobaltomenite originated from Parco Mine, Thompson's District, Grand County, Utah, USA and from El Dragon Mine, Potosi, Bolivia. Minerals associated with schmiederite in the El Dragon Mine deposit are chalcomenite, clinochalcomenite, ahlefdite, selenides as well as a number of other minerals. The composition of schmiederite was reported by Anthony *et al.*⁵.

Raman microprobe spectroscopy

The crystals of schmiederite were placed and orientated on the stage of an Olympus BHS microscope, equipped with 10x and 50x objectives as part of a Renishaw 1000 Raman microscope system, which also includes a monochromator, a filter system and a Charge Coupled Device (CCD). Raman spectra were excited by a HeNe laser (633 nm) at a resolution of 2 cm^{-1} in the range between 100 and 4000 cm^{-1} . Repeated acquisition using the highest magnification was accumulated to improve the signal to noise ratio. Spectra were calibrated using the 520.5 cm^{-1} line of a silicon wafer.

Spectroscopic manipulation such as baseline adjustment, smoothing and normalisation were performed using the Spectralcalc software package GRAMS (Galactic Industries Corporation, NH, USA). Band component analysis was undertaken using the Jandel 'Peakfit' software package, which enabled the type of fitting, function to be selected and allows specific parameters to be fixed or varied accordingly. Band fitting was done using a Gauss-Lorentz cross-product function with the minimum number of component bands used for the fitting process. The Gauss-Lorentz ratio was maintained at values greater than 0.7 and fitting was undertaken until reproducible results were obtained with squared correlations of r^2 greater than 0.995. Further details on the manipulation of the data has been published^{10,11,14,16,18,22,23,26-28}.

RESULTS AND DISCUSSION

Farmer states that very little research has been undertaken on selenates. No minerals with the selenate ion SeO_4^{2-} have been discovered and reported²⁹. Selenates are rather rare - only three are known: olsacherite, schmiederite and carlosruizite. Each of these minerals has two anionic groups: selenate and selenite (schmiederite), selenate and sulphate (olsacherite), and selenate and iodate (carlosruizite)³⁰. The infrared spectra of $\text{CuSeO}_3 \cdot 2\text{H}_2\text{O}$ has been reported by Sathinadan *et al.*³¹ and Makutan *et al.*³². Farmer reports that the band positions of selenates are readily distinguished from that of selenites. The selenite ion should show a maximum of six bands. The free ion will have C_{3v} symmetry and four modes, $2A_1$ and $2E$. Nakamoto³³ gives these as $807, 432\text{ cm}^{-1}$ (A_1) and $737, 374\text{ cm}^{-1}$ (E). Many studies of the selenate ion have been made^{34,35}. The position of the symmetric stretching mode occurs at lower wavenumbers than that of the antisymmetric stretching bands. The comment may be made, that there is very little published on the vibrational spectroscopy of selenite or selenate minerals, especially the Raman spectroscopy of these minerals.

The Raman spectrum of schmiederite in the 110 to 1110 cm^{-1} region is shown in Figure 2. Two bands are observed at 1095 and 934 cm^{-1} and are assigned to the antisymmetric and symmetric mode of the $(\text{SeO}_4)^{2-}$ anions. The infrared spectrum of schmiederite is reported in Figure 1S (supplementary information). The spectrum shows a broad profile with a significant number of overlapping bands. Two bands are observed at 1027 and 952 cm^{-1} which may correspond to the Raman bands. The advantage of Raman spectroscopy is the excellent band separation. For selenites, the symmetric stretching mode occurs at a higher position than the antisymmetric stretching mode³⁶, as is evidenced in the Raman spectrum of Figure 2. No comparison can be made with published data due to a lack of previous studies of natural occurring selenate minerals.

The band at 834 cm^{-1} is assigned to the symmetric $(\text{SeO}_3)^{2-}$ units. The two bands at 764 and 739 cm^{-1} are attributed to the antisymmetric $(\text{SeO}_3)^{2-}$ units. In the infrared spectrum (Figure 2S), two bands may be observed at 806 and 883 cm^{-1} which correspond to the antisymmetric and symmetric vibrations of the $(\text{SeO}_3)^{2-}$ units. The values of ν_1 for sodium, calcium and copper selenites are at 788 , 784 and 774 cm^{-1} . In contrast, the values for the ν_3 antisymmetric stretching mode occur at 740 , 713 and 714 cm^{-1} respectively. The value for ν_2 bands occurs between 449 and 461 cm^{-1} and ν_4 bands between 387 and 427 cm^{-1} ³⁶. Bäumer *et al.* proved that in the case of infrared spectra of M^{2+} selenite monohydrates, the stretching vibrations of selenite units are located in the regions $760 \leq \nu_1 \text{ SeO}_3 \leq 855\text{ cm}^{-1}$ and $680 \leq \nu_3 \text{ SeO}_3 \leq 775\text{ cm}^{-1}$ ³⁷. Khandelwal and Verma, and Verma assigned observed Raman and infrared bands for $(\text{NH}_4)_2(\text{UO}_2)_2(\text{SeO}_3)_3 \cdot 6\text{H}_2\text{O}$ at 384 , 390 (395), 475 (498), 731 and 829 (700 and 830), and 800 (808) cm^{-1} to the ν_4 , ν_2 , ν_3 and ν_1 modes, respectively, and those at 879 and 883 (872), and $(900)\text{ cm}^{-1}$ to the ν_1 and ν_3 $(\text{UO}_2)^{2+}$ modes, respectively^{38,39}.

The Raman spectrum of schmiederite in the 1300 to 2100 cm^{-1} region and the infrared spectrum in the 1200 to 1700 cm^{-1} region are shown in Figures 3 and 3S respectively. A number of sharp Raman bands are observed. Raman bands are observed at 1349 , 1418 , 1457 , 1576 and 1604 cm^{-1} . According to Effenberger⁹ the Pb(1) atoms in schmiederite each have 3 Pb-O bonds with bond lengths $<2.45\text{Å}$ with trigonal pyramidal arranged ligands; the Pb(2) atom in the schmiederite mineral has only 1 such near O atom. The Cu atoms are approximately square planar coordinated by the four hydroxyl groups. In addition, two further O atoms complete the coordination complex to give a very strongly distorted octahedron. The two bands at 1576 and 1604 cm^{-1} are assigned to the deformation modes of the OH units. The observation of multiple OH bands supports the concept of a much distorted structure based upon the four OH units coordinating the copper in a square planar structure. This brings into question the molecular model as shown in Figure 1. Such a model is based upon single crystal XRD data. Raman spectra suggest the molecular model is a lot more distorted than is displayed in Figure 1. The two broad bands at 1852 and 1919 cm^{-1} are assigned to combination bands of the selenate units. In the infrared spectrum, a broad spectral profile is observed which may be decomposed into component bands at 1347 , 1379 , 1410 , 1468 , 1490 and 1518 cm^{-1} . The first three bands are assigned to the diamond cell. The latter three bands are attributed to the infrared vibrations of the OH units in the schmiederite structure.

A previous study gave the values for ν_2 bands for selenite ion at 449 and 461 cm^{-1} and the ν_4 bands occurring between 387 and 427 cm^{-1} ³⁶, where the band at around 472 cm^{-1} is attributed to ν_2 bending mode. An intense sharp band at 398 cm^{-1} for schmiederite is assigned to this ν_2 bending mode. Some variation in band position is observed for clinocalcomenite where the band is found at 489 cm^{-1} . Two bands are observed for cobaltomenite at 512 and 443 cm^{-1} . The latter band is assigned to the ν_2 bending mode. Bands are observed at 367 and 396 cm^{-1} for chalcomenite and 349 , 361 and 378 cm^{-1} for clinocalcomenite. These bands are ascribed to the ν_4 bending mode.

The Raman spectrum of the OH stretching region is displayed in Figure 4. A single symmetric band is observed at 3428 cm^{-1} and is attributed to the OH stretching

vibration of the OH units in the schmiederite structure. The observation of a single band is in harmony with the observation of the deformation modes as observed in Figures 3 and 2S. The Raman band at 1604 cm^{-1} may be due to the water HOH bending mode. The band is observed at 1634 cm^{-1} in the infrared spectrum. The observation of a single symmetric stretching mode in the Raman spectrum suggests that all of the OH units are equivalent. More complexity is observed in the infrared spectra (Figure 3S). A series of bands are found at 2746 , 2878 and 2921 cm^{-1} . These bands are assigned to CH stretching vibrations and arise from impurities. OH stretching vibrations are observed at 3150 , 3383 and 3525 cm^{-1} . The observation of multiple OH stretching bands supports the concept of non-equivalent OH units in the schmiederite structure. The difference in the number of bands in the OH stretching region between the Raman and infrared spectrum may be explained in terms of symmetry. The vibrational modes which are highly symmetric will be Raman active and those which are non-symmetric are infrared active.

CONCLUSIONS

Raman spectroscopy lends itself to the studies of selenites and selenates and related minerals. Two Raman bands are observed at 1095 and 934 cm^{-1} and are assigned to the symmetric and antisymmetric mode of the $(\text{SeO}_4)^{2-}$ anions. For selenates and selenites the symmetric stretching mode occurs at a higher position than the antisymmetric stretching mode³⁶, as is evidenced in the Raman spectrum of schmiederite. The band at 834 cm^{-1} is assigned to the symmetric $(\text{SeO}_3)^{2-}$ units. The two bands at 764 and 739 cm^{-1} are attributed to the antisymmetric $(\text{SeO}_3)^{2-}$ units. An intense sharp band at 398 cm^{-1} for schmiederite is assigned to the ν_2 bending mode.

The two bands at 1576 and 1604 cm^{-1} are assigned to the deformation modes of the OH units. The observation of multiple OH bands supports the concept of a complex distorted structure based upon the four OH units coordinating the copper in a square planar structure. A single symmetric Raman band is observed at 3428 cm^{-1} and is assigned to the symmetric stretching mode of the OH units. The observation of multiple infrared OH stretching bands supports the concept of non-equivalent OH units in the schmiederite structure.

Acknowledgements

The financial and infra-structure support of the Queensland University of Technology Inorganic Materials Research Program of the School of Physical and Chemical Sciences is gratefully acknowledged. The Australian Research Council (ARC) is thanked for funding.

References

1. Dana, JD *Dana's Manual of Mineralogy*, by W. E. Ford. 13th edition, entirely revised and rewritten.
2. Mandarino, JA. *European Journal of Mineralogy* 1994; **6**: 337.
3. Mandarino, JA. *American Mineralogist* 1964; **49**: 1481.
4. Robinson, PD, Sen Gupta, PK, Swihart, GH, Houk, L. *American Mineralogist* 1992; **77**: 834.
5. Anthony, JW, Bideaux, RA, Bladh, KW, Nichols, MC *Handbook of Mineralogy*; Mineral Data Publishing: Tuscon, Arizona, USA, 2000; Vol. 4.
6. Campostrini, I, Gramaccioli, CM. *Neues Jahrbuch fuer Mineralogie, Abhandlungen* 2001; **177**: 37.
7. Hawthorne, FC. *Zeitschrift fuer Kristallographie* 1990; **192**: 1.
8. Sarp, H, Burri, G. *Schweizerische Mineralogische und Petrographische Mitteilungen* 1987; **67**: 219.
9. Effenberger, H. *Mineralogy and Petrology* 1987; **36**: 3.
10. Frost, RL, Cejka, J, Weier, M, Martens, WN. *Journal of Raman Spectroscopy* 2006; **37**: 879.
11. Frost, RL, Weier, ML, Reddy, BJ, Cejka, J. *Journal of Raman Spectroscopy* 2006; **37**: 816.
12. Frost, RL, Henry, DA, Weier, ML, Martens, W. *Journal of Raman Spectroscopy* 2006; **37**: 722.
13. Frost, RL, Weier, ML, Cejka, J, Klopogge, JT. *Journal of Raman Spectroscopy* 2006; **37**: 585.
14. Frost, RL, Weier, ML, Martens, WN, Klopogge, JT, Kristof, J. *Journal of Raman Spectroscopy* 2005; **36**: 797.
15. Frost, RL, Dickfos, MJ. *Journal of Raman Spectroscopy* 2007; **38**: 1516.
16. Frost, RL, Cejka, J. *Journal of Raman Spectroscopy* 2007; **38**: 1488.
17. Locke, AJ, Martens, WN, Frost, RL. *Journal of Raman Spectroscopy* 2007; **38**: 1429.
18. Frost, RL, Cejka, J, Ayoko, GA, Weier, ML. *Journal of Raman Spectroscopy* 2007; **38**: 1311.
19. Frost, RL, Bouzaid, JM. *Journal of Raman Spectroscopy* 2007; **38**: 873.
20. Frost, RL, Pinto, C. *Journal of Raman Spectroscopy* 2007; **38**: 841.
21. Frost, RL, Weier, ML, Williams, PA, Leverett, P, Klopogge, JT. *Journal of Raman Spectroscopy* 2007; **38**: 574.
22. Frost, RL, Cejka, J, Weier, ML. *Journal of Raman Spectroscopy* 2007; **38**: 460.
23. Frost, RL, Cejka, J, Weier, ML, Martens, WN, Ayoko, GA. *Journal of Raman Spectroscopy* 2007; **38**: 398.
24. Frost, RL, Bouzaid, JM, Martens, WN, Reddy, BJ. *Journal of Raman Spectroscopy* 2007; **38**: 135.
25. Frost, RL, Palmer, SJ, Bouzaid, JM, Reddy, BJ. *Journal of Raman Spectroscopy* 2007; **38**: 68.
26. Frost, RL, Cejka, J, Weier, M, Ayoko, GA. *Journal of Raman Spectroscopy* 2006; **37**: 1362.
27. Frost, RL, Cejka, J, Weier, ML, Martens, W. *Journal of Raman Spectroscopy* 2006; **37**: 538.
28. Frost, RL, Henry, DA, Erickson, K. *Journal of Raman Spectroscopy* 2004; **35**: 255.
29. Farmer, VC *Mineralogical Society Monograph 4: The Infrared Spectra of Minerals*, 1974.
30. Krivovichev, VG, Depmeier, W. *Zapiski Rossiiskogo Mineralogicheskogo Obshchestva* 2005; **134**: 1.
31. Sathianandan, K, McCorry, LD, Margrave, JL. *Spectrochimica Acta* 1964; **20**: 957.
32. Makatun, VN, Pechkovskii, VV, Mel'nikova, RY, Gusev, SS. *Zhurnal Prikladnoi Spektroskopii* 1970; **12**: 497.
33. Nakamoto, K *Infrared Spectra of Inorganic and Coordination Compounds. 2nd ed.*, 1970.
34. Eysel, HH, Wagner, R. *Spectrochimica Acta, Part A: Molecular and Biomolecular Spectroscopy* 1993; **49A**: 503.
35. Schulze, H, Weinstock, N, Mueller, A, Vandrish, G. *Spectrochimica Acta, Part A: Molecular and Biomolecular Spectroscopy* 1973; **29A**: 1705.
36. Ross, SD *Inorganic Infrared and Raman spectra*; McGraw-Hill: London, 1972.
37. Baeumer, U, Boldt, K, Engelen, B, Mueller, H, Unterderweide, K. *Zeitschrift fuer Anorganische und Allgemeine Chemie* 1999; **625**: 395.
38. Khandelwal, BL, Verma, VP. *Journal of Inorganic and Nuclear Chemistry* 1976; **38**: 763.
39. Verma, VP. *Thermochimica Acta* 1999; **327**: 63.

List of Figures

Figure 1 Model of schmiederite structure

Figure 2 Raman spectrum of schmiederite in the 110 to 1110 cm^{-1} region.

Figure 3 Raman spectrum of schmiederite in the 1300 to 2100 cm^{-1} region.

Figure 4 Raman spectrum of schmiederite in the 3350 to 3500 cm^{-1} region.

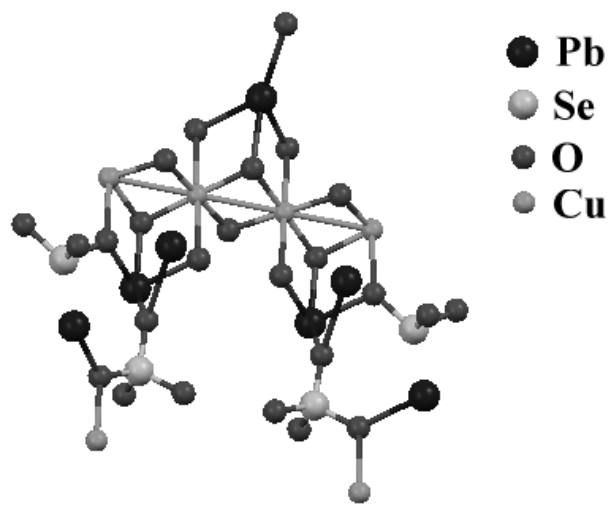


Figure 1

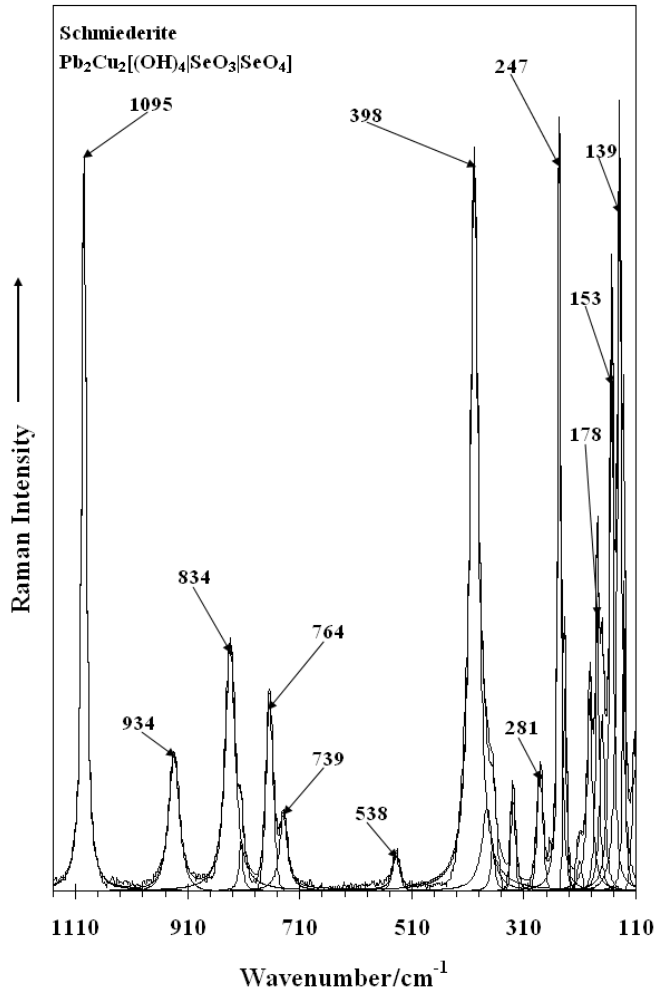


Figure 2

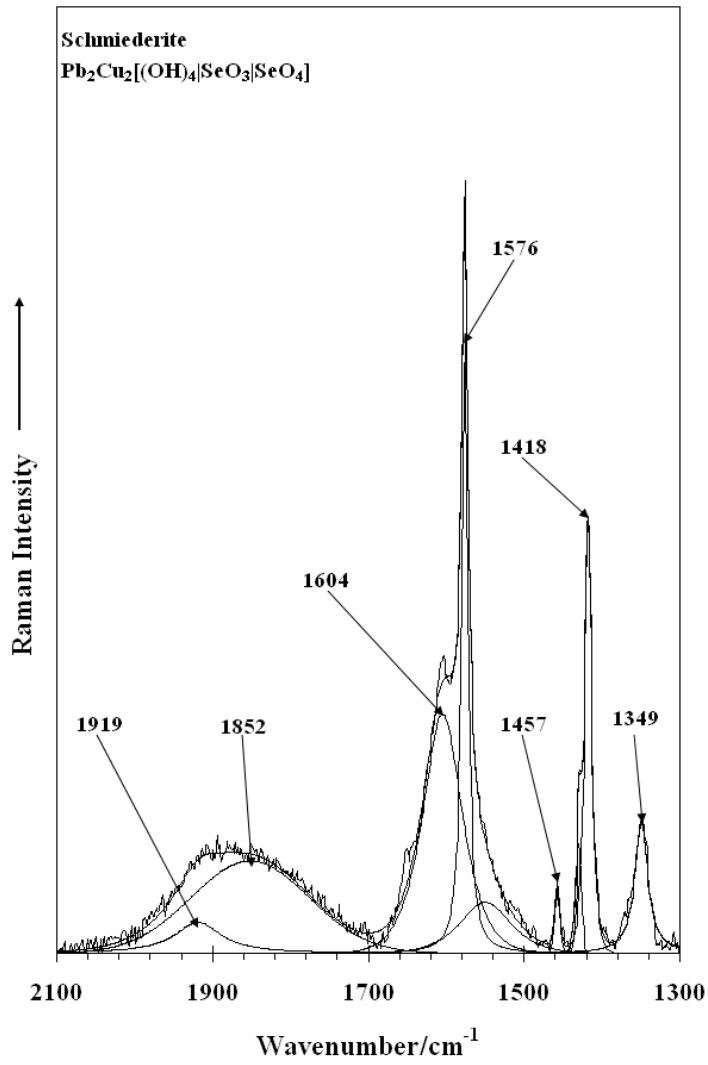


Figure 3

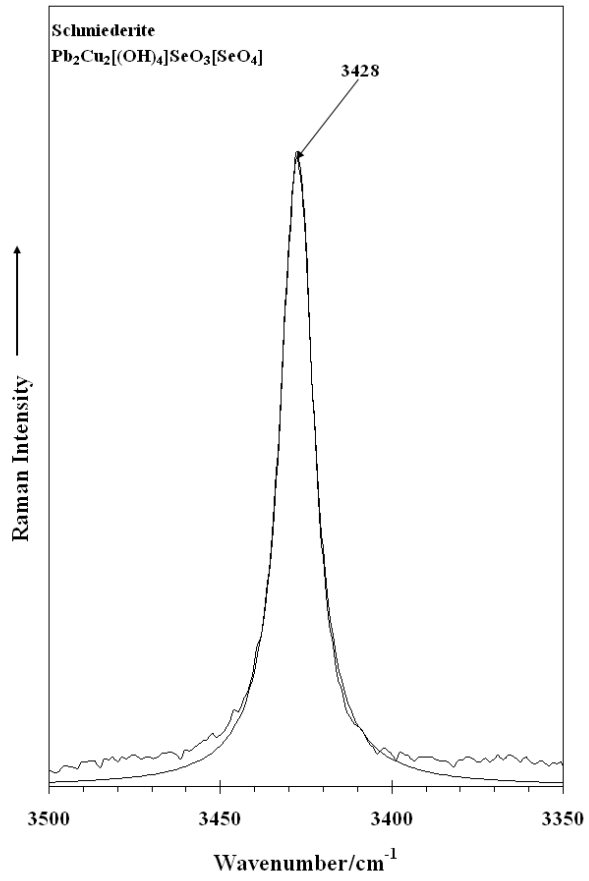


Figure 4